Spectroscopic characterization of the CeO$_2$/TiO$_2$ and Rh–CeO$_2$/TiO$_2$ systems: CO adsorption and NO–CO, NO–C$_3$H$_8$ reactions

E. Guglielminotti *, F. Boccuzzi

Department of Inorganic, Physical and Materials Chemistry, University of Turin, Via P. Giuria 7, 10125-Torino, Italy

Abstract

The activity of Rh supported on the ceria doped titania was investigated by FTIR technique using CO and NO adsorption. The addition of ceria does not lead to new adsorbed species: however the difficult reduction at 500 K of chloride ions of impregnated Rh salt and the persistence of Rh^{1+} sites until 773 K are the fingerprints of the effects of ceria addition which favours the rhodium dispersion. At 773 K the reduced catalyst becomes conductive and loss its IR transparency, that is recovered at RT by adsorption of O$_2$ and NO: the latter is easily dissociated already at RT and reacts with CO producing a full conversion to N$_2$ and CO$_2$ at 473 K. In absence of oxygen, propane is partially oxidised at 573 K to CO and CO$_2$ species, whereas NO is reduced to N$_2$ and NH$_x$ surface groups.

Keywords: FTIR; Carbon monoxide; Nitric oxide adsorption; Rhodium; Supported catalysts; Ceria; Titania

1. Introduction

The literature has recently reserved increasing attention to the systems utilized in the catalytic converters of automotive exhausts. The goal was the improvement of the catalysts which convert CO and residual hydrocarbons of exhausts to CO$_2$ and contemporary NO$_x$ to N$_2$ without formation of NH$_3$.

The more promising and practically used catalytic converters are based on Pt, Pd and Rh supported on alumina with the addition of ceria to enhance the catalytic performances [1–4]. The main functions proposed for ceria are: (i) the improvement of the thermal stability of the support; (ii) the stabilization of the dispersion of noble metals and (iii) the oxygen storage from the NO$_x$ decomposition during the transient operating conditions.

The TPD results of Rh/CeO$_2$ catalyst show a very strong metal–support interaction (SMSI), an oxygen migration at low temperature (≤ 400 K) and an easy NO$_x$ dissociation [4]. The primary activity of Rh seems to catalyse the NO$_x$ removal from exhausts which occurs at temperatures significantly lower than on Pt.

The comparison of turnover number and activation energy for the NO–CO reaction catalyzed by rhodium on different supports revealed that the support had only a minor effect on the reaction kinetics [5]. Therefore supports different from aluminas, as titania, could be utilized to support

* Corresponding author.

Rh in the NO_x removal. The SMSI effect was extensively demonstrated to occur on the Rh/TiO_2 system reduced at high temperature (≈ 773 K) [6,7]: in these conditions a reduction of the support, with formation of a non stoichiometric TiO_x phase spreading on the metal seems to occurs. The coating by the support is an undesired effect because it reduces the rhodium exposure and its activity in NO decomposition; however the reduced titania can itself contribute to the NO dissociation [6]: the addition of ceria with its function of oxygen storage could partially retard the reductive agglomeration of Rh^{1+} to Rh^0 and therefore maintain an high Rh dispersion.

The data here presented concern the study, mainly by FTIR spectroscopic experiments, of the activity of rhodium supported on the CeO_2/TiO_2. Carbon monoxide is used as test molecule of this system reduced at low (500 K) and high (773 K) temperature. The NO adsorption and the NO + CO reaction were followed by IR and mass spectroscopic experiments. Finally a survey experiment of reactivity between NO and propane was performed in situ. By comparison with the literature data, the effects of ceria addition to Rh/TiO_2 will be discussed.

2. Experimental

The CeO_2/TiO_2 (CeO_2 4% mole) was prepared by the incipient wetness method, with impregnation of a $Ce(NO_3)_3 \cdot 6H_2O$ solution (from Aldrich) with a Degussa P.25 TiO_2 support, dried 2 h at 373 K and then calcined 1 h at 573 K at the atmosphere.

The same impregnation method was utilized to prepare the Rh–CeO_2/TiO_2 catalyst from a $RhCl_3$ solution (Aldrich) with the previously prepared CeO_2/TiO_2 support and containing 1% wt of Rh. The $RhCl_3$ solution was acid by HCl at pH ≈ 3 in order to avoid the formation of the $CeTiO_3$ phase with perovskite structure formed in basic medium [8]. The amorphous sample is dried at the atmosphere 8 h at 373 K and then submitted to different thermal and oxoreducing treatments.

The BET areas of the samples are not very different from that of the P.25 TiO_2 support, i.e. ≈ 50 m^2/g.

Gases of very high purity ($\geq 99.9\%$) from Union Carbide were used without purification, except NO which was freshly distilled before the use.

The FTIR spectra were recorded by a Perkin Elmer 1760 instrument equipped with a data station and MCT cryodetector and operating with 2 cm^{-1} resolution. The spectra were run at room temperature (RT) and reported in absorbance after the background subtraction: some are shifted in the baseline to eliminate the strong changes in the background transparency after the thermal and chemical treatments of the samples (see Discussion).

The mass spectroscopic data were obtained by a VG Micromass 100 instrument connected to the IR cell through a needle valve.

3. Results and discussion

3.1. CO adsorbed on CeO_2/TiO_2

In Fig. 1 are reported the FTIR spectra of CO adsorbed at RT on the CeO_2/TiO_2 support submitted to different thermal and chemical treatments. Fig. 1A shows the spectra of CO adsorbed on the sample oxidized 20 min and outgassed 2 h at 573 K. At this temperature the stoichiometry of both CeO_2 and TiO_2 should be maintained under vacuum; the water, on the contrary, is fully eliminated from the surface with only small amount of residual titania hydroxyls remaining onto the surface, as shown in the νOH region 3750–3600 cm^{-1} [9]. The spectrum of the sample contacted with 24.8 mbar CO (curve a) shows only two maxima at 2206 and 2187 cm^{-1}; curve b is the spectrum of CO at a pressure lowered to 3 mbar; if the pressure is further lowered to 1.10^{-2} mbar the weakly adsorbed CO is fully eliminated (curve c) and also the rotational contour of the CO gas in the low frequency side completely disappears.
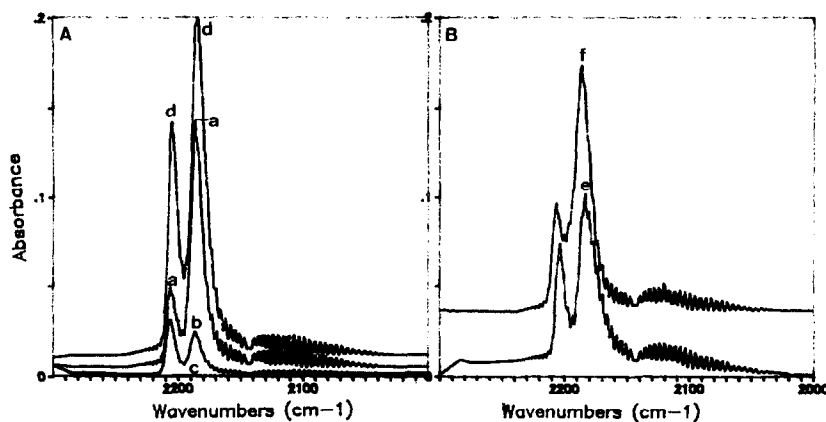
Fig. 1. Comparison of CO adsorbed at RT on CeO$_2$(4% mole)/TiO$_2$ submitted to different thermal and chemical treatments. A, sample oxidised 20 min and outgassed 2 h at 573 K; curve a: contacted with 24.8 mbar CO; curves b and c: CO pressure 3 and 1 × 10^{-2} mbar, respectively; curve d: 28 mbar CO adsorbed on the sample oxidised 20 min and outgassed 2 h at 673 K. B, curve e: 29.5 mbar CO adsorbed at RT on the sample H$_2$ reduced 2 h and outgassed 15 min at 673 K; curve f: 25.2 mbar CO adsorbed on the sample H$_2$ reduced 2 h at 773 K, contacted with 6 mbar O$_2$ at RT and evacuated to 1 × 10^{-2} mbar pressure.

In curve d is reported the spectrum of CO adsorbed at 28 mbar on the same sample, oxidized 20 min and outgassed 2 h at 673 K. The spectrum is similar to that of the sample evacuated at 573 K, with an increase in intensity mainly of the band at 2206 cm^{-1}. For the spectral frequency and the behaviour on outgassing the 2187 cm^{-1} band can be attributed to CO species weakly chemisorbed on coordinatively unsaturated (cus) Ti^{4+} ions of an extended TiO$_2$ surface. A lower hydroxyls environment and highly unsaturated sites as kinks and corners are supposed for CO adsorbed at 2206 cm^{-1} [9].

Fig. 1B, curve e, shows the spectrum of 29.5 mbar CO contacted with the same sample, reduced for 2 h and outgassed for 15 min at 673 K. The intensity of the band at 2187 cm^{-1} is particularly depressed and the frequencies of the maxima are red shifted by ≈ 3 cm^{-1} with respect to that of the sample oxidized to the same temperature. If the sample is reduced for 2 h and outgassed for 15 min at 773 K its transparency in the IR region, already lowered by reduction at 673 K, becomes nil. This is the fingerprint of a more profound reduction of the oxidic supports, because both the TiO$_2$ [10] and the CeO$_2$ [11] in these conditions are depleted of oxygen and become n-type semiconductors with loss of transparency. However, as already observed [10], the contact of few mbar

of oxygen (or of an oxidising gas as N$_2$O or NO) at RT is sufficient to partially restore the stoichiometry and the quite significant transparency of the sample. If O$_2$ is evacuated after contact at RT and then CO is allowed to the surface at a 25.2 mbar pressure, the spectrum of curve f is obtained. The band at 2187 cm^{-1} is increased in intensity without change in frequencies.

A contribution from CO adsorbed on ceria cannot be excluded for the broader band centered at 2187 cm^{-1}: two weak bands at 2177 and 2156 cm^{-1} were found for CO adsorbed on ceria outgassed at 1000 K [12]; however the high temperature of our treatments (773 K) is much lower than 1000 K and no other bands are found, as in [12], in the low frequency region of the spectrum.

After reduction at 773 K the sample becomes completely opaque in the IR region, but a brief contact at RT with O$_2$, followed by evacuation of the gas phase, is sufficient to partially restore the transparency. The CO adsorption on this mildly oxidised sample leads (Fig. 2) to the activated formation of broad weak bands at 1586–1548, 1325sh–1300, 1175 cm^{-1}, increasing with the time of contact. The frequencies of these bands and their formation when the sample was pre-contacted with oxygen, are in agreement with their assignment to surface carbonate or carboxylate species [13]; the assignment of the bands at 1300
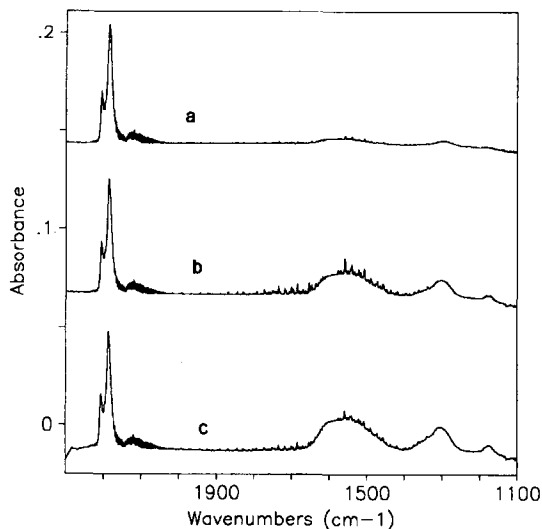
Fig. 2. CO adsorption at RT on the sample treated as in Fig. 1, curve f. Curves a, b and c: 25.2 mbar CO adsorbed, spectrum recorded after 1, 30 and 60 min respectively.

and 1175 cm^{-1} to CO_2^{2-} carbonite species, as hypothesized by Lavalley et al. on ceria [14], cannot be excluded. The $CO_2^{\delta-}$ is formed by CO interacting with an oxygen near a defect of ceria [11] or at the titania–ceria interface, following the mechanism:
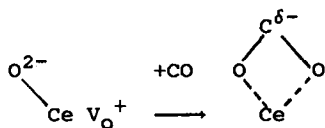
The complexes of CO_2 with alkali metals (C_{2v} symmetry) show two IR bands in the same spectral region [13,14]: the charge is indicated as $\delta-$ for the n-semiconducting nature of the support. The bands at 1585, 1413, 1310 and 1220 cm^{-1} are the same as that shown by CO_2 adsorbed on titania [15] except the last which is typical of the δOH mode of a bicarbonate species and correlated to the bands at 1580 and 1413 cm^{-1}. The absence of this band in our spectrum excludes this species; the components at 1586 and 1325 cm^{-1} can be therefore tentatively assigned to bidentate carbonate on titania.

3.2. CO adsorption on Rh–CeO₂/TiO₂

Fig. 3 shows the spectra of CO adsorbed at RT on 1%Rh–CeO₂/TiO₂ sample oxidised for 15

min, reduced with H_2 for 1 h and outgassed for 15 min at 500 K. The spectra show that the adsorbed CO is slightly increasing with the pressure for the curves a, b, c, corresponding to 0.4, 4.1, and 18.2 mbar CO respectively. Curve d shows the spectrum at RT of the adsorbate remaining after heating in the CO atmosphere for 15 min at 500 K. The band increasing with the CO pressure at 2187 cm^{-1} was already assigned to CO weakly adsorbed on one type of Ti^{4+} cus sites [9].
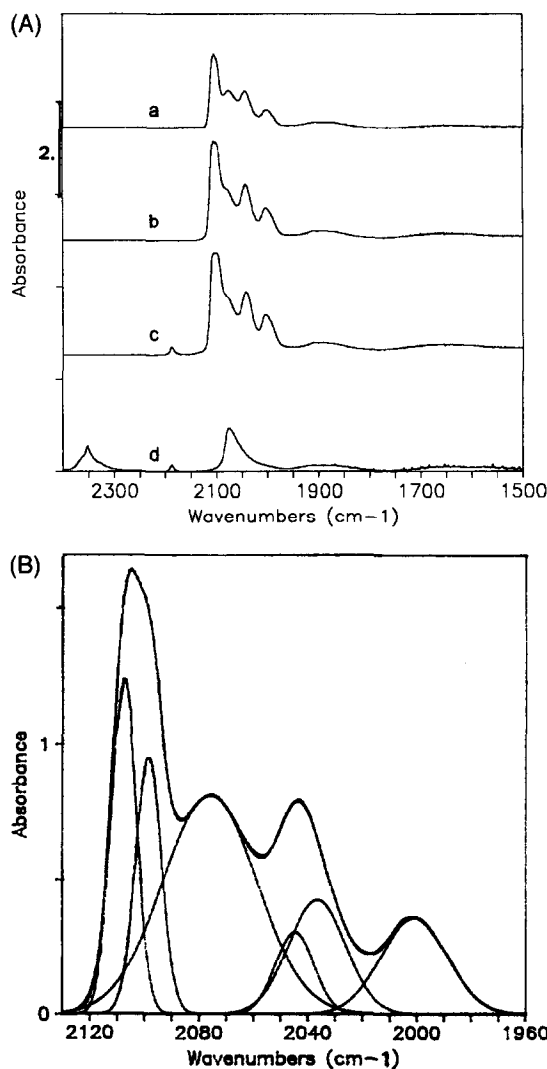

Fig. 3. CO adsorbed at RT on 1%Rh–CeO₂/TiO₂ oxidised 15 min, H₂ reduced 60 min and outgassed 15 min at 500 K. (A) curves a, b and c: CO pressure 0.4, 4.1 and 18.2 mbar, respectively; curve d: after heating in 10.4 mbar CO 15 min at 500 K. (B) curve-fit with six gaussian peaks of the spectrum shown in A, curve b.

The band at 2075 cm^{-1} is assigned to CO linearly adsorbed on Rh^0 and is accompanied by the weak and broad bands at 1912–1875 cm^{-1} assigned to CO bridged onto Rh^0 microcrystals [16]. This assignment is supported by the consideration that these bands remain, although slightly shifted in frequencies, after reduction at 500 K in CO with formation of linearly adsorbed CO$_2$ at 2350 cm^{-1} (curve d). On the contrary, the bands which disappear after this treatment, i.e. those at 2105, 2044 and 2002 cm^{-1}, may be assigned to CO adsorbed on slightly oxidized Rh^{1+} sites [17–21].

The coupled bands at 2105 and 2044 cm^{-1} were usually assigned to Rh^{1+}(CO)$_2$ νCOasym. and sym. modes respectively, whereas a question arises on the assignment of the band at 2002 cm^{-1}. This band is absent or present only as a weak shoulder on the Rh/TiO$_2$ catalyst prepared ex RhCl$_3$ and reduced with a final outgassing under UH-vacuum conditions [21] or on the sample reduced at higher temperature (e.g. 773 K, see Fig. 5). This band is present also on the samples prepared by RhCl$_3$ impregnation on alumina [18] and on titania supports [19]. Its presence can therefore be correlated, in agreement with [19], to Rh^{1+} ions linked, for an insufficient reduction at 500 K, to residual chloride ions. The difficult elimination of chloride ions during the preparation of supported metals ex chlorides is well known in literature for Ru [22] and Rh [6,19] supported on titania. This important problem therefore deserves further considerations. In Ref. [19] the band at 2005 cm^{-1} is assigned to Rh$_2^{1+}$–CO bridged species, intermediate in the disruption of Rh crystallites by CO.

Fig. 4 shows that on the sample reduced by CO at 500 K (curve a) only the Rh^0–CO species remain (linear at 2075 and bridged at ≈ 1900 cm^{-1}). The evacuation at 300, 423 and 500 K (curves b, c, d respectively) strongly lowers the concentration of the Rh^0–CO species, the frequency of the linear species shifting to 2072, 2058 and 2042 cm^{-1}. The red-shift of frequency with the decreasing coverage is certainly due to the decrease of dipole–dipole coupling effects of
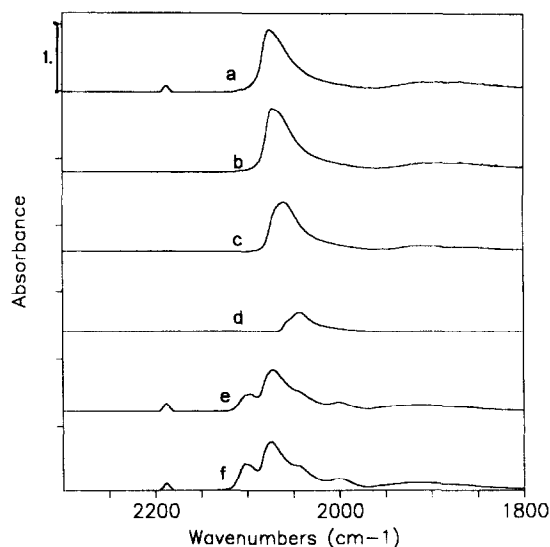

Fig. 4. CO adsorbed at RT on the 1%Rh–CeO$_2$/TiO$_2$ sample H$_2$ reduced at 500 K and heated 15 min in 10.4 mbar CO pressure at 500 K (curve a); curves b, c, d: after 15 min evacuation at 300, 423, 500 K, respectively; curve e: the sample of curve d recontacted with 10.4 mbar CO, immediately and, curve f, after 30 min, respectively.

adsorbed CO [23]. As a consequence CO re-adsorption (curves e, f) restores the intensity of the peaks at 2076 and ≈ 1900 cm^{-1}. However the peaks at 2105, 2044 and 2002 cm^{-1} are only partially restored: in particular, the 2105 cm^{-1} broad band reveals a dual peak structure and is lowered in intensity together with the bands at ≈ 2040 and 2002 cm^{-1}. The lower intensity of all these bands is in agreement with the reducing activity of the previous treatments, but the changes in the relative intensity need further discussion. The resolution of the envelope of bands between 2105 and 2000 cm^{-1} was achieved with the help of a computer curve fit program with gaussian curves. The resolution of several spectra of CO adsorbed at different coverages after different treatments was performed and is not reported here in detail for the sake of brevity; as an example, the resolution of curve b of Fig. 3 is shown in a magnified scale (Fig. 3B) with the best curve-fit obtained with six peaks. The figure clearly shows a perfect curve fit with the experimental data. In the following the numbers in parenthesis quote the FWHM of the bands: the absorption at ≈ 2100 cm^{-1} is composed by two narrow peaks at 2107.6 (11.0), 2098.5 (11.5) and by four bands at 2076 (41.7),
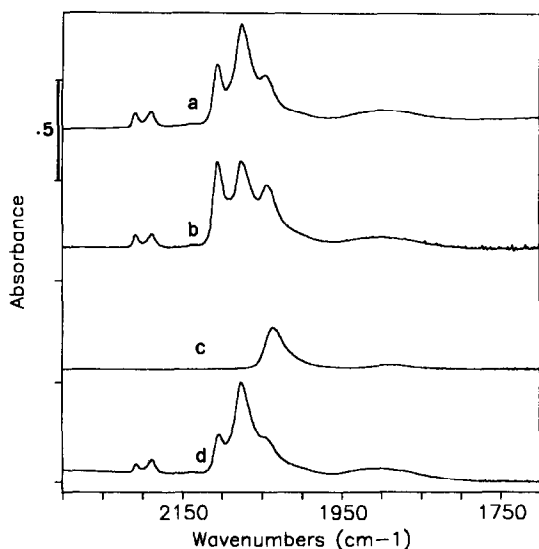
Fig. 5. CO adsorbed at RT on the 1%Rh–CeO$_2$/TiO$_2$ sample H$_2$ reduced 1 h at 773 K. Curves a and b: 10 mbar CO contacted 1 and 30 min respectively; curve c: sample of curve b outgassed 1 h at 500 K; curve d: 6.8 mbar CO readsorbed on the sample of curve c.

2044.8 (16.9), 20.6 (25.3) and 2000.9 (29.0) cm^{-1}. The broadness of the component due to Rh^0–CO at 2076, shifting to 2079 cm^{-1} with the increasing coverage, is not surprising for a CO species adsorbed on an heterogeneously dispersed metal. A good fitting is however obtained also with a five peaks curve-fit, showing a substantial constancy in the spectroscopic features of the first three peaks, a fourth peak at 2041.3 (25.0) cm^{-1} and a fifth peak at 2001.8 (31.0) cm^{-1}.

A slightly poorer fitting is obtained with a four peaks model, fitting the high frequency band with only one peak centered at 2103.7 cm^{-1} (17.3); the frequencies and FWHM of the other bands are practically constant. For the sake of simplicity, it is possible to make the assignment of the bands between 2130 and 1960 cm^{-1} an the basis of a four peak model with the caution that the band at ≈ 2100 cm^{-1} is surely composed of two peaks and the same is probably valid also for the band at ≈ 2042 cm^{-1}. The assignment is carried out with the help of the data concerning the same wafer, reported in Fig. 3, Fig. 4 (CO adsorbed on the sample reduced by CO at 500 K) and Fig. 5 (CO adsorbed on the sample reduced at 773 K). In Table 1 are reported the total integrated areas

and the four peaks areas of CO adsorbed at full coverage on the sample reduced at 500 and 773 K. By increasing the reduction temperature, the total area decreases by a factor 0.19, the integrated area of the peak of CO on the metal at 2076 cm^{-1} decreases by a factor 0.24 while the peak at ≈ 2002 cm^{-1} strongly decreases by a factor 0.08: the decrease of total integrated areas after high temperature reduction indicates a sintering or a decoration effect of the metal particles, but the Rh^0 phase increases relatively with the temperature of reduction. The band at 2002 cm^{-1}, in agreement with the literature [18,19] can be correlated to an Rh$_2^+$–CO species with rhodium oxidised by residual chloride ions, strongly decreasing with the increase of the temperature of reduction. The bands at ≈ 2103 and ≈ 2042 cm^{-1} are assigned to Rh^{1+}(CO)$_2$ surface complexes on sites with slightly different environments for the two peaks fine structure. The frequency and the relative intensity of the two bands strongly depends from the angle between the CO ligands and from the environment of the Rh sites (OH residual groups, interaction with the support etc.) [17–21,24,25]. On the basis of a simple vectorial model it is possible to calculate the angle formed between the Rh^{1+} and the two CO groups by the ratio of the integrated intensity of the two bands, as for heterogeneous [24] and homogeneous complex [26]: the evaluated angle is 100° 20 for the sample reduced at 500 K, but it increases to 102° 40 for the sample reduced at 773 K. This result is reasonable because the Rh$^+$ sites, formed by oxidative interaction of Rh with the residual hydroxyls of the support [21,25], at 773 K are exposed to a cleaner surface and a wider angle is

Table 1
Areas of adsorbed CO at saturation, range 2130–1960 cm^{-1}

Treatments	Reduced at 500 K	Reduced at 773 K	Area ratios: 773/500
Total area	132.8	25.0	0.19
2076 peak	42.4	10.2	0.24
2002 peak	20.2	1.6	0.08
2103 peak	39.0	5.0	0.13
2042 peak	31.2	8.2	0.26

allowed to the CO ligands. Because the angle of the $Rh^{1+}(CO)_2$ species changes with the temperature of reduction, also the integrated areas of the two peaks at ≈ 2103 and ≈ 2042 cm^{-1} are lowered by different factors, i.e. 0.13 and 0.26 respectively; the ratio between the single value of these areas and the area of the peak at 2076 cm^{-1} is therefore meaningless, but the mean decrease of the species roughly parallels the reduction of total area by sintering or decoration of the metal particles: we can therefore advance the hypothesis that the correlated species are formed at the borderline of the Rh^0 microcrystals.

After reduction at 773 K the residual transparency of the background is very low ($T\%$ max. ≈ 7 versus ≈ 70 of the same sample reduced at 500 K) and becomes almost nil for a prolonged reduction process, probably for a deeper reduction of TiO_2 and CeO_2, already observed in literature [10,11,22]. On the sample partially reduced, both at 500 and at 773 K, the contact with CO at RT further reduces the transparency by a slow activated process, following roughly an Elovich kinetics.

On the samples well reduced or reduced at 500 K by CO itself the transparency changes induced by CO adsorption become nil. A contact of the reduced sample with oxygen at RT quickly restores a high transparency because the free electrons are trapped as O_2^- species on the support [10]. The same effect is shown by other oxidising reactants as NO and N_2O decomposed on defective sites.

Fig. 5, curve a, shows the spectrum of CO adsorbed on the sample reduced 1 h at 773 K; curve b shows also an increase, for prolonged contact with CO, of the coupled bands at 2103 and 2042 cm^{-1}, whereas the intensity of the band at 2036 cm^{-1} is slightly lowered. This behavior can be understood if a conversion from Rh^0–CO to $Rh^{1+}(CO)_2$ species, produced by a CO dismutation and/or by reaction with residual hydroxyls, is hypothesized [17,21,25]. The oxidised Rh^{1+} species are fully eliminated by outgassing 30 min at 500 K (curve c); this treatment leaves a residual Rh^0–CO band at 20 cm^{-1}, red shifted for the

reduction with the coverage of the effect of dipole dipole coupling [23]. CO readsorption at RT (curve d) completely restores the Rh^0–CO band at 2076 cm^{-1} and the bridged CO band at ≈ 1900 cm^{-1}; the peaks at 2103 and 2042 cm^{-1} are formed with minor intensity probably because of the reducing effect of the previously adsorbed CO. These experiments shows therefore that the relative concentration of the surface CO species bound to Rh^0 and Rh^{1+} on various supports are a complex function of the temperatures and times of the reducing treatments mainly for the ex-chloride samples, the time of contact with CO, the residual H_2O and OH groups of the different supports etc.; this accounts for the great variety of CO frequencies and intensities given in literature for these bands.

Apparently the ceria does not changes this scenario: its presence and its aptitude to store oxygen may increase the difficulty to reduce the metal to Rh^0, as shown by the relative high intensity of the bands correlated to the Rh^{1+} species even after high temperature reduction. We may therefore hypothesise the stabilization of the higher dispersion of Rh, which favours (see the following part) the NO dissociation [6].

3.3. NO–CO reaction

This experiment was carried out on a sample reduced at 773 K. As discussed in the previous section, the H_2 reduction 2 h at 773 K followed by 15 min evacuation at the same temperature leads to a sample completely dark at RT in the IR region. However the contact with 5.3 mbar of freshly distilled NO produces, by a slow activated process at RT, a continuous increase of the transparency, reaching the plateau after ≈ 30 min. Nitric oxide dissociates with formation of N_2O and adsorption of oxygen as O^- or O^{2-} species and trapping of electrons from the reduced support that recovers the transparency.

Fig. 6 shows the spectra in absorbance without background subtraction for the lack of a reference background before NO adsorption. Two quite intense bands at 2242 and 2235 cm^{-1} (curve a)

are easily assigned to weakly chemisorbed N_2O: the formation of N_2O is promoted by the Ti^{3+} and Ce^{+3} sites formed after reduction at 773 K [10,11,27]: the reduced support is therefore cooperating in NO dissociation. The broad bands at 1912, 1828 and 1750–1675sh cm^{-1} are similar to those previously found on other supported Rh samples [28]. These bands, relative to NO adsorbed on different Rh sites, are not found by NO adsorption at low temperatures on the Rh faces, as (111), of Rh monocrystals; the EELS spectroscopy shows at low temperatures and coverages the νNO of the undissociated molecule at ≈ 1480 cm^{-1}, shifting to 1630 cm^{-1} at higher coverages [29]. Besides, at RT and at high coverages the NO dissociation is well documented and is accompanied by IR bands at 1840 and 1750 cm^{-1} [16,29,30]; these bands are formed also by NO adsorbed on a Rh surface pre-contacted with O_2 [29] and therefore can be assigned to NO on a Rh site with adjacent oxygen atoms. The assignment of the 1828 and 1750 cm^{-1} bands is therefore based on this assignment; the band at 1912 cm^{-1}, which shows a different chemical and thermal behaviour (see the following discussion), is assigned to an oxidised NO_x ($x>1$) species or to NO bound to Rh^{1+} [28].

Fig. 6, curve b, shows that NO interaction with CO at RT (ratio CO:NO ≈ 3) nearly completely eliminates the bands at 1912 and 1828 cm^{-1} of NO adsorbed on the more oxidised Rh sites; the broad band at 1750 cm^{-1} is partially eroded at RT leaving a band centered at 1734 cm^{-1} and a shoulder at 1675 cm^{-1}. Also the N_2O component at 2242 cm^{-1} is eroded and CO (weakly adsorbed on Ti^{4+} cus sites at 2207 and 2190 cm^{-1}) is partially oxidised to CO_2 (linearly adsorbed at 2350 cm^{-1}). The oxidation of CO is also proved by the appearance of bands of carbonates species at 1582 and 1350–1300 cm^{-1}; strong bands of CO adsorbed on oxidised Rh^{1+} at 2104 and 2040 cm^{-1} are formed. A shoulder band at ~2125 may be assigned to CO adsorbed on a more oxidised Rh^{+3} site [18].

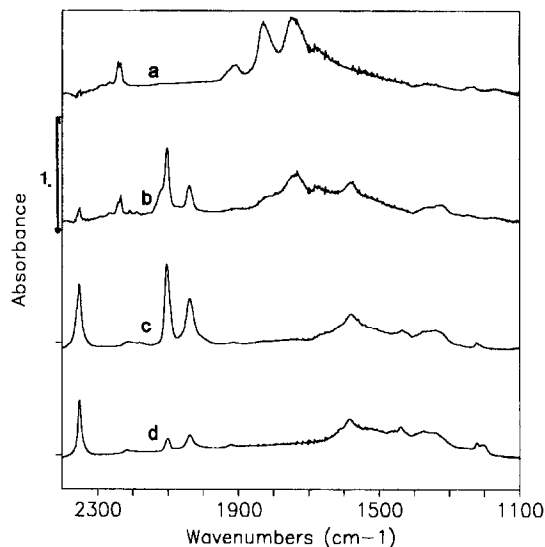The NO–CO mixture that remains for 3 days in the cell shows the spectrum changes as in Fig. 6,

Fig. 6. NO adsorption at RT and CO/NO = 3 mixture reaction up to 473 K. Curve a: NO adsorbed at 5.3 mbar initial pressure; curve b: after 5 mbar CO contact (CO/NO ≈ 3 mixture determined by mass spectroscopy), immediately; curve c: after 3 days; curve d: the same of curve c, after heating 20 min at 473 K.

curve c. The elimination of residual adsorbed NO species at 1734 cm^{-1} with the oxidative attack to CO is accomplished: the N_2O species disappear and the CO_2 species at 2350 cm^{-1} strongly increases together with the CO groups linked to Rh^{1+} at 2104–2040 cm^{-1}. This behaviour is similar to that of NO adsorbed on Rh–Ce/Al_2O_3 [5,31]: the addition of cerium produces an enhancement of the NO dissociation rate at quite low temperatures and suppresses the N_2O formation.

New bicarbonate species are formed, probably by a slow process of diffusion of water from the wall of the cell to the catalyst wafer; these species are related to the bands at 1223 (bicarbonate δOH), 1435 and to a component at ≈ 1580 cm^{-1} [13]. The weak and broad bands at 2213 and 2165 cm^{-1} may be assigned for their frequency [28] and behaviour to the thermal treatment (see curve d) to isocyanates chemisorbed on the titania and on the Rh phase respectively. Curve d shows that, after heating at 473 K in presence of the CO > NO mixture, some $Rh^{1+}CO)_2$ species remains in the spectrum and therefore that Rh^{1+} is reduced with difficulty to Rh^0. As a matter of fact the band at 2040 cm^{-1} shows a higher intensity than the 2105

cm^{-1} one, contrary to that shown in the curves b and c and this can be ascribed to the presence in curve d of a weak Rh^0–CO component at ≈ 2040 cm^{-1}. The difficult reducibility is different from that usually shown by supported Rh [28] and is related to the dispersive and oxidising action of ceria on Rh in the reaction conditions. The bicarbonate bands slightly increase by heating at 473 K; at the same time the Rh–isocyanate species fully reacts and the Ti–isocyanates partially resist at this temperature.

In these conditions (473 K) the mass spectroscopic data shows the presence in the residual reacting mixture only of $m/e = 28$ (N_2,CO) and 44 (CO_2, for the absence of N_2O at the IR) species: the CO–NO reaction, forming N_2 and CO_2 in mild temperature conditions, is therefore accomplished. Because CO is prevailing in the reactive mixture, the $Rh^{1+}(CO)_2$ bands decrease by reduction at 473 K, but Rh^0 is formed with difficulty.

In conclusion, ceria favours the dispersion of rhodium which seems to be more active in the NO–CO reaction, giving N_2 and CO_2 at quite low temperature, as desired in the catalytic converters. In presence of ceria, the NO reduction proceeds by means of a transient and easily reactive N_2O intermediate which lowers the temperature of NO conversion.

3.4. NO–C$_3$H$_8$ reaction

The experimental data reported in Fig. 7 are referred to a sample reduced for 2 h at 773 K, i.e initially dark in the IR region before the NO adsorption. Curve a shows NO adsorbed at the equilibrium, after 30 min and the spectrum is identical to that shown in Fig. 6, with formation of N_2O species. The parallel mass spectroscopic data show the prevailing of the $m/e = 30$ peak (NO) accompanied by weak peaks at $m/e = 44$ (N_2O), 28 (N_2) and 32 (O_2). The mixture with C_3H_8 was followed by the $m/e = 29$ main peak, starting from an initial C_3H_8/NO ≈ 2 ratio at RT.

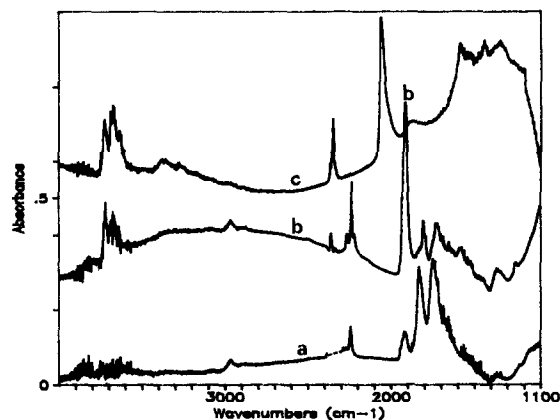Fig. 7, curve a, shows the broad and weak band at 2960 cm^{-1} of propane in the initial mixture,

Fig. 7. Propane/NO $\approx$ 2 mixture adsorbed at RT and heated until 573 K in the cell. Curve a: after 20 min at RT; curves b and c: after heating 20 min at 473 K and 573 K, respectively.

unchanged by the mixture with NO. After heating 20 min at 473 K (curve b) the main changes on the spectrum are: (i) the increase of νOH groups at 3725–40 cm^{-1}; (ii) the weak increase of CO_2 linearly adsorbed species at ≈ 2350 cm^{-1}; (iii) the increase of N_2O species, in particular that of the component at 2245 cm^{-1}, plus a weak band at 2265 cm^{-1}, tentatively assigned to N_2O bound to Rh^{1+} through an O dative bond [32]; (iv) the strong increase of the band at 1916 cm^{-1}. The strong increase of the band at 1916 cm^{-1} was found for NO adsorbed on supported Rh treated in the same way [28] and is therefore not specific of our system; it occurs at the expense of the bands of adsorbed NO at 1830–1750 cm^{-1} which decrease in intensity and red shift with the maxima at 1805–1800 and 1726 cm^{-1}. Weak bands at 1580, 1248 cm^{-1} can be assigned to bidentate nitrate species spilled over into the support [33]. The weak band at 1360 cm^{-1} is of uncertain assignment. The band remaining at 2960 cm^{-1} shows that the propane is only slightly reactive at 473 K. The reactivity shown by IR is confirmed by the mass spectroscopic data; they show a slight decrease of the C_3H_8 principal peak intensity with respect to the RT mixture, the decrease of $\approx 1/3$ of the NO concentration and a concomitant increase of $m/e = 44$ peak ($N_2O + CO_2$). The absence of linear CO_2 and carbonates species together with the increase of the 2245 cm^{-1} band

at the IR shows that this peak is due mainly to N_2O.

After heating at 473 K, the oxidative NO decomposition is testified, besides the increase of the N_2O and Rh^{1+}–NO (1916 cm^{-1}) bands by the strong increase of transparency of the sample. This shows the partial NO decomposition, with oxidation and partial stoichiometric restoring of the reduced support.

An opposite behaviour is shown after heating the NO–C_3H_8 mixture at 573 K. In this case a reductive reaction with decomposition of propane prevails. Curve c confirms the reducing action of the propane shown by: (i) the complete elimination of adsorbed NO at 1830–1675 cm^{-1}; (ii) the formation of CO bound to Rh^0 as linear (2058 cm^{-1}) and bridged (1890 cm^{-1}) species; (iii) the further enhancement of the bands at 3725–3640 cm^{-1} (surface OH groups) and 3360–3277 cm^{-1} (NH_x groups formed by a strong reduction of NO); (iv) the nearly full elimination of the propane absorption at 2960 cm^{-1} accompanied by the strong increase of the band at 2350 cm^{-1} (CO_2) and of carbonate bands between 1590 and 1300 cm^{-1}.

The spectroscopic data are confirmed by the mass spectra showing, after the treatment at 573 K, the full elimination of the $m/e = 30$ (NO) peak and the strong increase of the $m/e = 28$ ($N_2 + CO$) and $m/e = 44$ (CO_2) peaks; at the same time the $m/e = 29$ main peak of propane is practically eliminated. Therefore at 573 K the reduction of NO by propane is practically accomplished.

4. Conclusions

The CeO_2/TiO_2 support was investigated by CO adsorption for sake of comparison with supported Rh: the oxidation–reduction treatments between 573 and 773 K show the formation of active Ti^{4+} sites weakly adsorbing CO at 2206 and 2187 cm^{-1}; the last band may probably have the contribution of CO species adsorbed on cerium sites. Only after oxygen contact some carbonate, carboxylate and perhaps carbonite-like species are

formed by CO at RT with the participation of the surface ceria phase.

The Rh–CeO_2/TiO_2 system is apparently not very different from Rh/TiO_2, except for the more difficult reduction of chloride ions at 500 K and the persistence of Rh^{1+} sites at 773 K.

On this system CO is adsorbed on the metallic phase at 2076 cm^{-1} and on the Rh^{1+} sites preferentially, with formation of bicarbonylic species absorbing at 2103 and 2042 cm^{-1} and of monocarbonyl group at 2002 cm^{-1}. Mainly on the sample reduced at 500 K, but also on the sample reduced at 773 K, CO adsorption shows that the percent of Rh oxidized species is relatively high and is favored by the presence of the ceria with transfer of oxygen at low temperatures from the ceria to the highly dispersed Rh phase.

The main differences between the sample reduced at 500 or at 773 K, i.e. in SMSI conditions, are the decrease of the total Rh surface exposed, the relative increase in the Rh^0–CO species and the strong decrease in the transparency of the n-semiconducting support: the transparency of the support can be restored by O_2 adsorption.

The NO adsorption has the same function of O_2 in the elimination of the SMSI state: NO is quickly dissociated at RT on the Rh^0 assisted by the defective support, producing N_2, N_2O and O_2 species oxidising the metal. The oxidised Rh adsorbs NO forming species easily reactive at 300–473 K with CO: at the last temperature the reaction to CO_2 and N_2 is nearly accomplished with a small concentration of isocyanate species spilled over into the support. The easy migration of the oxygen formed by NO dissociation is probably favored by the presence of the ceria phase which keeps rhodium well dispersed.

A survey experiment of NO–propane reaction shows that at 573 K propane is oxidised partially to CO and to CO_2 with formation of N_2 and surface NH_x groups.

Acknowledgements

References

[1] J.T. Kummer, J. Phys. Chem., 90 (1986) 4747.

[2] B. Harrison, A.F. Diwel and C. Hallett, Platinum Met. Rev., 32 (1988) 73.

[3] K.C. Taylor, Catal. Rev.-Sci. Eng., 35 (1993) 457.

[4] G.S. Zafiris and R.J. Gorte, J. Catal., 139 (1993) 561; ibid., 143 (1993) 86 and references therein.

[5] S.H. Oh and C.C. Eickel, J. Catal., 128 (1991) 526.

[6] G. Munuera, A.R. Gonzales-Elipe, J.P. Espinos, A. Muñoz, J.C. Conesa, J. Soria and J. Sanz, Catal. Today, 2 (1988) 663.

[7] G.L. Haller and D.E. Resasco, Adv. Catal., 36 (1989) 173.

[8] A. Dauscher, P. Wehrer and L. Hilaire, Catal. Lett., 14 (1992) 171.

[9] C. Morterra, J. Chem. Soc., Faraday Trans. I, 84 (1988) 1617.

[10] F. Boccuzzi, E. Guglielminotti and G. Spoto, Surf. Sci., 251–252 (1991) 1069.

[11] F. Bozon-Verduraz and A. Bensalem, J. Chem. Soc., Faraday Trans., 90 (1994) 653.

[12] C. Li, Y. Sakata, T. Arai, K. Domen, K. Maruya and T. Onishi, J. Chem. Soc., Faraday Trans. I, 85 (1989) 929.

[13] G. Busca and V. Lorenzelli, Mater. Chem., 7 (1982) 89.

[14] C. Binet, A. Badri, M. Boutonnet-Kizling and J.C. Lavalley, J. Chem. Soc., Faraday Trans., 90 (1994) 1023.

[15] C. Morterra, A. Chiorino, F. Boccuzzi and E. Fisicaro, Z. Phys. Chem. NF, 124 (1981) 211; E. Guglielminotti, unpublished results.

[16] L.H. Dubois and G.A. Somorjai, Surf. Sci., 91 (1980) 514; L.H. Dubois, P.K. Hansma and G.A. Somorjai, J. Catal., 65 (1980) 318.

[17] F. Solymosi and M. Pásztor, J. Phys.Chem., 89 (1985) 4789; ibid., 90 (1986) 5312 and references therein.

[18] C.A. Rice, S.D. Worley, C.W. Curtis, J.A. Guin and A.R. Tarrer, J. Chem. Phys., 74 (1981) 6487.

[19] Z.L. Zhang, A. Kladi and X.E. Verykios, J. Mol. Catal., 89 (1994) 229.

[20] J. Evans, B. Hayden, F. Mosselmans and A. Murray, Surf. Sci., 279 (1992) L159.

[21] D.A. Buchanan, M.E. Hernandez, F. Solymosi and J.M. White, J. Catal., 125 (1990) 456.

[22] G.C. Bond, R.R. Rajaram and R.J. Burch, J. Phys. Chem., 90 (1986) 4877; E. Guglielminotti and G.C. Bond, J. Chem. Soc., Faraday Trans., 86 (1990) 979.

[23] R.M. Hammaker, S.A. Francis and R.P. Eischens, Spectrochim. Acta, 21 (1965) 1295.

[24] H. Knözinger, E.W. Thornton and M. Wolf, J. Chem. Soc. Faraday Trans. I, 75 (1978) 1888.

[25] P. Basu, D. Ponayotov and J.J.,Jr Yates, J. Phys. Chem., 91 (1987) 3133.

[26] P.S. Braterman, Metal Carbonyl Spectra, Academic Press, London, 1975, p. 46.

[27] J.M. Schwartz and L.D. Schmidt, J. Catal, 148 (1994) 22.

[28] H. Arai and H. Tominaga, J. Catal., 43 (1975) 131; F. Solymosi and J. Sárkány, Appl. Surf. Sci., 3 (1979) 68; V. Rives-Arnau and G. Munuera, Appl. Surf. Sci., 6 (1980) 122; F. Solymosi, T. Bánsági and E. Novák, J. Catal., 112 (1988) 183.

[29] T.W. Root, G.B. Fisher and L.D. Schmidt, J. Chem. Phys., 85 (1986) 4679, 4687; J.S. Villarrubia and W. Ho, J. Chem. Phys., 87 (1987) 750.

[30] R.M. Wolf, J.W. Bakker and B.E. Nieuwenhuys, Surf. Sci., 246 (1991) 135.

[31] S.H. Oh, J. Catal., 124 (1990) 477.

[32] E. Borello, L. Cerruti, G. Ghiotti and E. Guglielminotti, Inorg. Chim. Acta, 6 (1972) 45.

[33] E. Guglielminotti F. Boccuzzi, J. Chem. Soc., Faraday Trans., 87 (1991) 337 and references therein.